Cell Death and Differentiation (2007) 14, 559–567

www.nature.com/cdd

XLX is an IAP family member regulated by phosphorylation during meiosis

J Greenwood[1] and J Gautier*[,2]

The balance between proliferation and cell death is critical for embryonic development and adult tissue homeostasis. Within an individual cell, coordination of these pathways is aided by direct communication between cell cycle factors and molecules that regulate apoptosis. Here, we show that XLX, a *Xenopus laevis* inhibitor of apoptosis (IAP) family member, exhibits characteristics typical of an IAP, such as caspase inhibition and autoubiquitylation. However, unlike other IAPs described thus far, we found that XLX is phosphorylated during meiosis by protein kinases that belong to the MAPK and MPF pathways. Finally, we show that caspase-dependent cleavage of XLX is altered when XLX is phosphorylated. In addition to furthering our understanding of the post-translational regulation of an IAP, these findings reveal a novel link between cell cycle-regulated protein kinases and a component potentially involved in apoptosis.
Cell Death and Differentiation (2007) **14,** 559–567. doi:10.1038/sj.cdd.4402031; published online 29 September 2006

The ability of the inhibitor of apoptosis (IAP) family of proteins to protect cells from death has been well documented.[1] The highly conserved baculoviral IAP repeat (BIR), found in 1–3 copies in every IAP, is the domain that mediates apoptosis inhibition, in some cases, through direct binding of caspases. In addition, many IAPs possess a C-terminal RING domain. This structural motif confers E3-ubiquitin ligase activity to IAPs allowing them to target numerous substrates, including IAPs themselves, caspases, IAP antagonists, and other cellular proteins, for polyubiquitylation. Many questions remain, however, regarding the *in vivo* functions and specific mechanisms employed by individual vertebrate IAPs in promoting survival. For example, whereas DIAP1 is essential in fly embryos, mice lacking XIAP show no obvious developmental defects.[2,3] The existence of at least eight mammalian BIR-containing proteins suggests that IAPs may have evolved individually unique antiapoptotic functions. Biochemical analyses have led to the identification of the residues in the BIRs of cIAP-1, cIAP-2, and XIAP responsible for caspase binding.[4–6] The absence of these residues in ML-IAP and ILP-2 can explain the poor *in vitro* caspase-inhibition activity of these IAPs.[7,8] It has therefore been hypothesized that some IAPs may act instead as protein sinks to bind proapoptotic proteins, such as IAP antagonists.[9–11] This could effectively protect a true caspase inhibitor, such as XIAP, from inhibition. The E3 ubiquitin ligase activity of IAPs could then aid in their function by promoting the polyubiquitylation and subsequent proteasomal degradation of bound proteins. Until the *in vivo* functions of individual vertebrate IAPs can be elucidated, we continue to rely on biochemical and cell culture studies to uncover mechanistic details regarding IAP function.

Much of the research on IAPs has focused on their inhibition of caspases, their expression in cancer cells, and their inhibition by IAP antagonists such as Smac/Diablo and Omi/HtrA2. There have been relatively few reports on the post-translational modification of IAPs other than ubiquitylation. Phosphorylation is widely used by many cellular signaling pathways, and also plays an important role in the regulation of cell death. One study found that when Ser87 of XIAP was phosphorylated by AKT, XIAP protein was stabilized.[12] However, phosphorylation does not universally protect IAPs from degradation. In fact, phosphorylation by the Hpo/Sav/Wts pathway seems to promote the degradation of DIAP1, although the phosphorylated residues have not been identified.[13,14]

Cells also regulate the activity of IAPs post-translationally through proteolytic cleavage. As with phosphorylation, the biological consequence of IAP cleavage varies. For example, cleavage of DIAP1 at Asp20 by effector caspase DrICE generates a more antiapoptotic form of DIAP1. Specifically, the newly exposed N-terminus of DIAP1 serves as a degron for the N-end rule degradation pathway.[15] The turnover of DIAP1 contributes to cell viability by taking along the bound caspase. In contrast, caspase-dependent cleavage of other IAPs can lead to inactivation of the IAP or even the generation of proapoptotic IAP fragments.[16–18]

Xenopus egg extracts have been instrumental in the investigation of apoptosis regulation.[19] Many of the features of programmed cell death can be recapitulated in this cell-free system, such as caspase activation, cytochrome *c* release from mitochondria, and DNA fragmentation. When crude extracts are incubated for a prolonged period, spontaneous release of cytochrome *c* from mitochondria occurs, triggering the caspase cascade. Furthermore, *Xenopus* egg extracts that undergo apoptosis can be made in a cell cycle stage-specific manner, thereby providing an experimental system in

[1]Integrated Program in Cellular, Molecular, and Biophysical Studies, Columbia University Medical Center, New York, NY 10032, USA and [2]Department of Genetics and Development, Columbia University Medical Center, Institute for Cancer Genetics, 1130 St. Nicholas Avenue, ICRC 603A, New York, NY 10032, USA
*Corresponding author: J Gautier, Genetics and Development, Columbia University Medical Center, Institute for Cancer Genetics, 1130 St. Nicholas Avenue, ICRC 603A, New York, NY 10032, USA. Tel: +1 212 851 4564; Fax: +1 212 923 2090; E-mail: jg130@columbia.edu
Keywords: IAP; apoptosis; MPF; MAPK; meiosis; *Xenopus*
Abbreviations: IAP, inhibitor of apoptosis; XLX, *Xenopus laevis* XIAP homolog; tPARP, truncated poly-ADP ribose polymerase
Received 19.4.06; revised 21.7.06; accepted 21.7.06; Edited by D Vaux; published online 29.9.06

which to study the coordination of these two cellular processes. It was reported that metaphase (CSF)-arrested extracts are more resistant to caspase activation than interphase extracts.[20,21] Surprisingly, the resistance observed in metaphase extracts is not due to enhanced 'mitochondrial stability', as cytochrome *c* release was detected at similar times in both extracts. Therefore, it appears that CSF-arrested extracts protect against caspase activation at a step downstream of cytochrome *c* release. These studies also demonstrated that the MAPK pathway is necessary for apoptotic resistance in CSF extracts, although the downstream target(s) has not been identified.

Here, we have characterized XLX, a *Xenopus laevis* member of the IAP family of proteins. We have found that XLX is uniquely modified by MAPK- and Cdc2/Cyclin B-dependent phosphorylation during oocyte maturation. We further demonstrate that XLX is cleaved in a caspase-dependent manner, and that phosphorylation of XLX alters the profile of cleavage products.

Results

G2-arrested oocytes are more susceptible to cytochrome *c*-induced caspase activation than oocytes undergoing meiosis. Previous studies have shown that resistance of CSF extracts to caspase activation occurs downstream of cytochrome *c* release and is dependent on MAPK activity.[20,21] We sought to determine whether immature G2-arrested oocytes, which lack MAPK activity, were more susceptible to caspase activation than metaphase II-arrested oocytes. Extracts were generated from G2- or metaphase II-arrested oocytes and recombinant cytochrome *c* was added at various concentrations. Caspase activity was monitored by the cleavage of ^{35}S-labeled truncated PARP (tPARP), a conserved caspase substrate.[22] Consistently, cytochrome *c*-dependent caspase activity was elevated in G2-arrested extracts compared to extracts made from metaphase II-arrested oocytes at all concentrations of cytochrome *c* (Figure 1a).

To determine whether the acquisition of apoptotic resistance correlated with the initiation of meiosis, and hence the activation of the MAPK and MPF pathways, we then examined the susceptibility of oocytes to cytochrome *c*-induced caspase activation throughout meiotic progression (Figure 1b). We found that apoptotic resistance is not restricted to metaphase II, but rather, is conferred at the time of nuclear envelope (germinal vesicle) breakdown, or GVBD, and coincides with the activation of the MAPK pathway. Consistent with previous studies, we find that metaphase II-arrested oocytes incubated with Ca^{2+} ionophore to mimic fertilization and M-phase exit, lost the resistance to apoptosis. Interestingly, histone H1 kinase activity, a measure of Cdc2/Cyclin B activity, was detected in activated oocytes, presumably owing to the re-entry into mitosis (Figure 1b, bottom panel). This observation provides further evidence that MAPK activity rather than MPF activity contributes to meiotic apoptotic resistance. These data suggest that an antiapoptotic factor is upregulated or that a proapoptotic factor is inactivated during oocyte maturation.

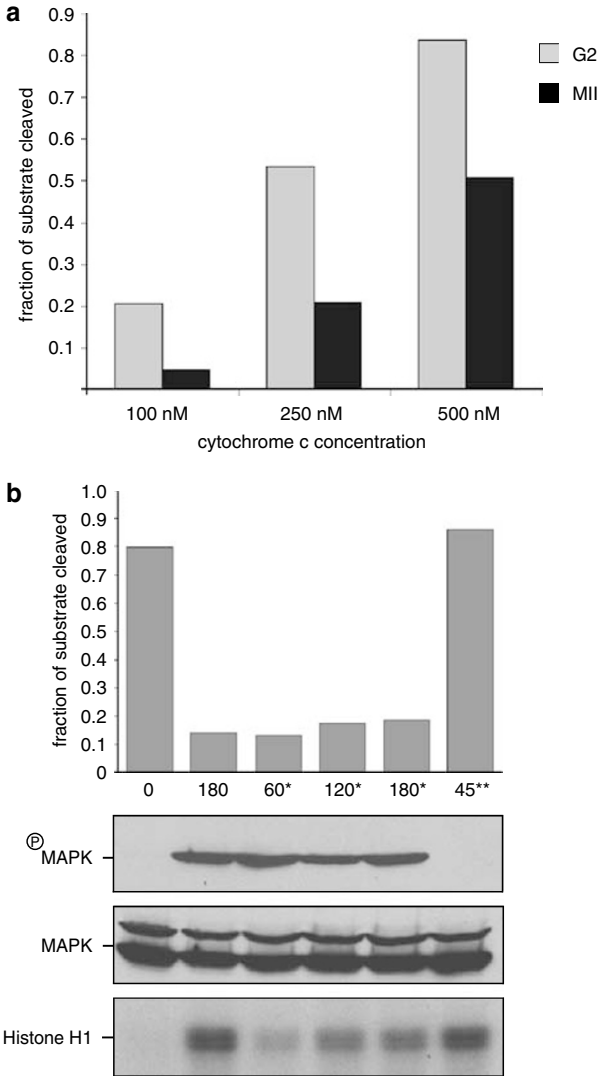

Figure 1 Metaphase II-arrested oocytes are more resistant to cytochrome *c*-induced caspase activation than G2-arrested oocytes. (**a**) Extracts were generated from immature G2-arrested (gray bars) or metaphase II-arrested (black bars) oocytes, and recombinant cytochrome *c* was added at the concentrations indicated. Caspase activity was detected by analyzing the cleavage of an exogenous caspase substrate, ^{35}S-tPARP, by SDS-PAGE followed by autoradiography. The fraction of substrate cleaved was determined by subtracting the quantitated amount of full-length substrate remaining, and normalizing for the total signal/lane. The fraction of substrate cleaved at $t = 40$ min is shown. (**b**) Extracts were generated as in (**a**) from G2-arrested oocytes ($t = 0$), or from oocytes treated with progesterone that had undergone GVBD. GVBD, which was determined visually by the appearance of a characteristic white spot, occurred at 180 min. GVBD-positive (*) oocytes were removed and incubated for the time indicated (60*, 120*, and 180*). Following metaphase II arrest, oocytes were treated with Ca^{2+}-ionophore and incubated for 45 min (45**). The fraction substrate cleaved was determined as in (**a**) and is plotted in the bar graph. Antibodies specific for the phosphorylated form of MAPK were used to detect the activation of the MAPK pathway (top panel), whereas MAPK antibodies detect both activated and non-activated MAPK (middle panel) and serves as a loading control. A non-specific band was also detected with the MAPK antibody. Histone H1 kinase activity was monitored as a readout of MPF activity (bottom panel)

XLX is expressed in oocytes and early embryos and exhibits antiapoptotic activity. To understand better the regulation of apoptosis in the oocyte and early embryo, we

searched for candidate *Xenopus* apoptosis inhibitors. We found an mRNA encoding a BIR-containing protein that was expressed only in the oocyte and early embryo (data not shown), and have subsequently cloned and characterized this putative IAP. XLX, also cloned by Kornbluth and co-workers,[23] was initially named for its homology to XIAP; however, a more similar *Xenopus* XIAP homolog has been identified recently.[24] Based on sequence homology, XLX has two N-terminal BIRs and a C-terminal RING domain.

Using affinity-purified polyclonal antibodies generated against full-length XLX, we examined the developmental expression pattern of XLX protein by Western blot analysis (Figure 2a). Notably, the expression of XLX protein coincides with the phase of apoptosis resistance present in the early embryo.[25] Specifically, XLX protein is detectable in unfertilized eggs (stage 0), through the cleavage stages (stages 2–8) and becomes nearly undetectable following gastrulation (stage 10.5).

Given its overall structure and its classification as an IAP, we sought to determine whether XLX could inhibit caspase activity. We took advantage of the fact that *Xenopus* embryos subjected to genotoxic insults undergo highly synchronous apoptosis at the onset of gastrulation, provided the damage was inflicted before the mid-blastula transition.[26–29] We generated caspase-active cell-free extracts from gastrulation stage embryos that had been treated at the four-cell stage with camptothecin, an inhibitor of DNA topoisomerase I that leads to the generation of double-strand breaks during DNA replication. Caspase activity was monitored by cleavage of ^{35}S-labeled truncated-PARP (^{35}S-tPARP).[22] Addition of peptide caspase inhibitor, DMQD, to these caspase-active extracts blocked the cleavage of ^{35}S-tPARP, whereas GST had no effect, thus confirming the specificity of the assay (Supplementary Figure 1a). We found that ^{35}S-tPARP cleavage was decreased 2.5-fold following addition of 1.6 μM recombinant GST-XLX to caspase active extracts, when compared to GST alone at $t = 10$ min (Figure 2c). The caspase-inhibition activity of XLX was dose-dependent (Supplementary Figure 1b). We also tested truncated versions of XLX (depicted schematically in Figure 2b) and found that the BIR2 domain alone (GST-XLXBIR2) was sufficient to inhibit caspase activity, whereas an N-terminal deletion lacking both BIR domains (GST-XLX214-400) was inactive in this assay (Figure 2c; Supplementary Figure 1b). GST-XLXΔR, a construct lacking the C-terminal RING domain, inhibited caspase activity as effectively as full-length XLX, suggesting that the putative E3 ubiquitin-ligase activity is dispensable for caspase inhibition in this assay.

To determine whether XLX exhibited other features characteristic of an IAP, we then investigated the *in vitro* autoubiquitylation activity of XLX. We used an XLX substrate lacking the RING domain, ^{35}S-T7-XLXΔR, added recombinant E1, E2, His-tagged ubiquitin, and then either full-length GST-XLXwt or GST-XLXΔR as the source of the E3. We noted slowly migrating forms of the substrate on SDS-PAGE when the full-length, but not the RING-deleted mutant, was used as an E3 (Figure 2d). We confirmed that these forms were due to ubiquitylation by Western blotting for the ubiquitin His-tag (data not shown). This experiment demonstrated that XLX has RING-dependent autoubiquitylation activity, and that the ubiquitylation can occur intermolecularly.

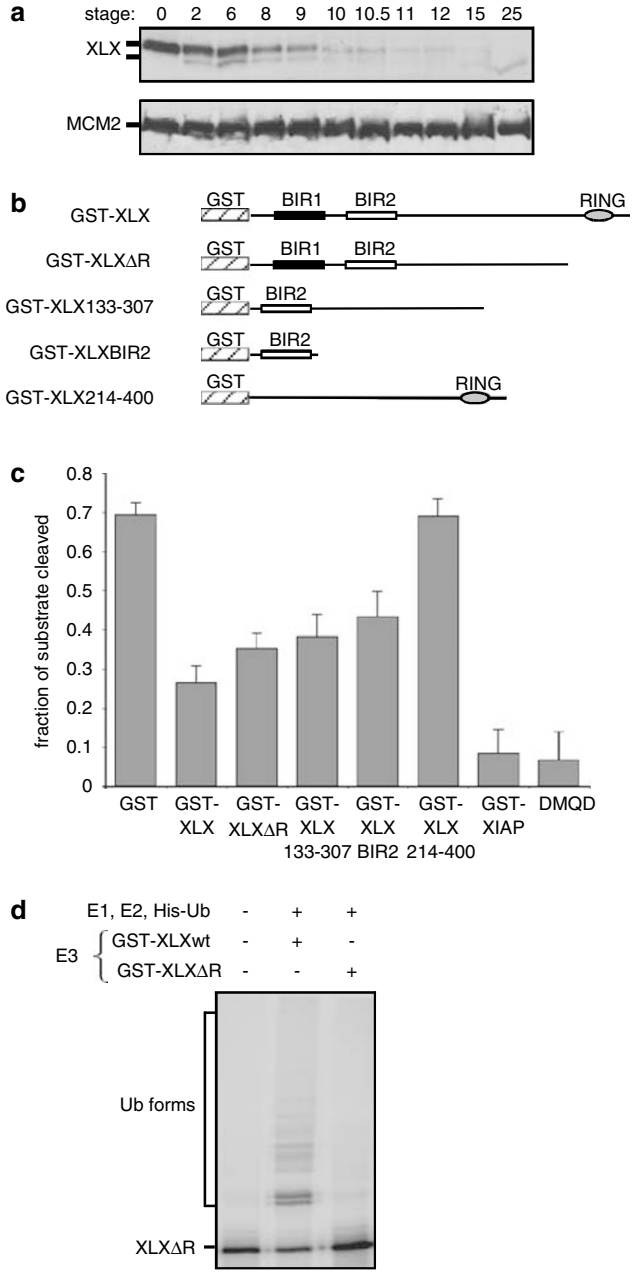

Figure 2 XLX exhibits antiapoptotic activity. (**a**) Developmental expression pattern of XLX was analyzed by Western blot using affinity-purified XLX-specific antibodies; the embryonic stage is indicated (top panel). MCM2 antibodies were used to confirm equal loading (bottom panel). (**b**) Structural domains of the constructs tested for caspase inhibition are represented schematically. (**c**) Caspase activity was quantitatively measured by monitoring cleavage of ^{35}S-tPARP. The fraction of substrate cleaved was determined as in Figure 1. Recombinant proteins (final concentration: 1.6 μM) were incubated in the caspase active extract just before the caspase substrate was added. The bar graph depicts the fraction substrate cleaved at $t = 10$ min. Error bars represent S.D. ($n = 7$). (**d**) An *in vitro* ubiquitylation reaction was conducted with recombinant E1, E2, His-Ub, and either GST-XLXwt or GST-XLXΔR as the E3. Ubiquitylation of the substrate, ^{35}S-T7-XLXΔR (XLXΔR), was monitored by SDS-PAGE followed by autoradiography

XLX is phosphorylated during oocyte maturation. Western blot analysis revealed an alternately migrating form of XLX in fertilized embryos (Figure 2a). We sought to determine whether the change in migration could be due to phosphorylation. Extracts were generated from unfertilized eggs arrested in metaphase of meiosis II, where we observe only the slower migrating form of XLX. Treatment of these extracts with recombinant protein phosphatase led to increased mobility of XLX protein on SDS-PAGE, thereby establishing that phosphorylation was the modification responsible for the observed shift (Figure 3a).

We then carried out a more detailed analysis of the phosphorylation of XLX during oocyte maturation to determine when the initial shift becomes detectable. XLX is present in its hypophosphorylated state in G2-arrested st. VI oocytes (Figure 3b, top panel, $t = 0$ min). Following induction of oocyte maturation by progesterone treatment, we observed XLX in its phosphorylated form at 180 min (Figure 3b, top panel), which coincided with GVBD and with activation of the MAPK and MPF pathways (Figure 3b, middle panel and graph, respectively).

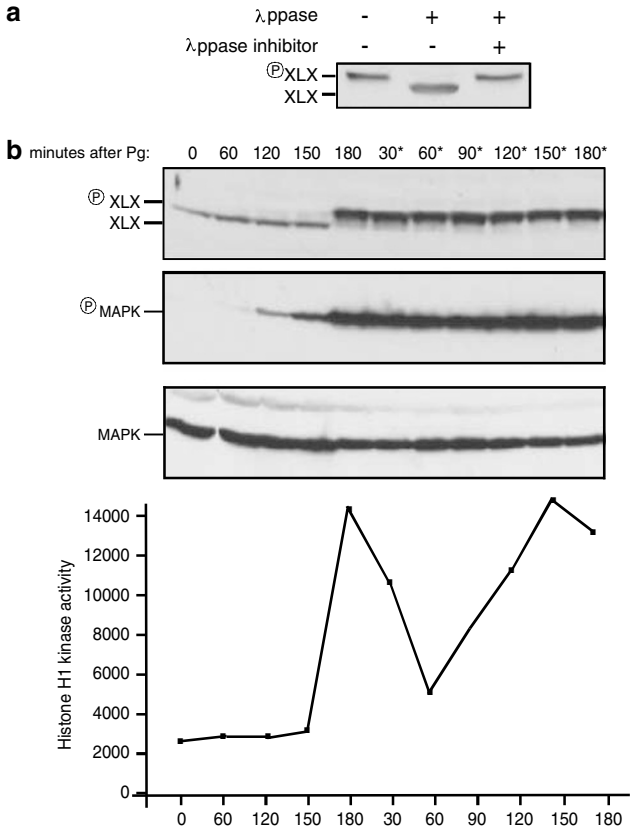

Figure 3 XLX is phosphorylated during oocyte maturation. (**a**) CSF extracts were treated with recombinant λ-phosphatase $+/-$ phosphatase inhibitors. The different forms of XLX were detected by Western blot using purified XLX antibodies. (**b**) Oocytes were collected at the indicated time points (minutes) following progesterone (Pg) addition, processed for SDS-PAGE, and analyzed by Western blot. GVBD took place at 180 min following progesterone addition. The time points (minutes) after GVBD are indicated with an asterisk (*). XLX phosphorylation was assayed by monitoring a mobility shift in XLX protein on SDS-PAGE followed by Western blot analysis with purified XLX antibodies (top panel). Antibodies specific for the phosphorylated form of MAPK were used to detect the activation of the MAPK pathway (middle panel), whereas MAPK antibodies detect both activated and non-activated MAPK (bottom panel) and serve as a loading control. Histone H1 kinase activity was monitored as a readout of MPF activity (graph)

The phosphorylation of XLX is MAPK-dependent. Given the concomitant activation of MAPK and XLX phosphorylation, we wanted to determine whether the MAPK pathway plays a direct role in the phosphorylation of XLX. First, we incubated oocytes undergoing meiotic maturation with U0126, a specific inhibitor of MEK, the upstream activating kinase of MAPK. As expected, U0126 blocked MAPK activation (Figure 4a, middle panel) but not MEK activation (Figure 4a, bottom panel). In addition, U0126 also prevented the complete mobility shift of XLX (Figure 4a, top panel). Cdc2/Cyclin B was activated at GVBD in both U0126-treated (240 min) and control oocytes (180 min); however, histone H1 kinase activity was lower in U0126-treated than in control oocytes following GVBD, as reported previously[30] (Figure 4a graph).

In a second approach, we used extracts derived from st. VI G2-arrested oocytes and ectopically activated the MAPK pathway using recombinant Mos protein. Addition of GST-Mos to st. VI extracts induced the expected activation of MAPK (Figure 4b, bottom panel) as well as a mobility shift of endogenous XLX (Figure 4b, top panel). This shift was not observed in the presence of U0126 (Figure 4b, top panel). Similarly, Mos induced a mobility shift of exogenous XLX (Figure 4c). An assay for histone H1 kinase activity confirmed that Cdc2/Cyclin B was not activated in these extracts (not shown). Taken together, these data establish that the MAPK pathway plays a direct role in the meiotic phosphorylation of XLX.

We then examined the protein sequence of XLX for potential MAPK phosphorylation sites. We identified a region following the second BIR domain that contained five serine-proline repeats. A T7-tagged XLX clone with all five of these serines mutated to alanines (T7-XLXS/A) was generated, mRNA from this clone and T7-XLXwt, were synthesized *in vitro* and injected into G2-arrested oocytes. Some of the injected oocytes were treated with progesterone to induce meiotic maturation. Using Western blot analysis with an antibody against the T7 tag, we observed that the change in mobility of T7-XLXwt following oocyte maturation was abrogated in the S/A mutant (Figure 5a). Next, we used this assay to examine the phosphorylation of mutants containing individual point mutations and various combinations of mutations and have found that only a mutant in which all five serines are mutated completely inhibits the shift of XLX (Supplementary Figure 2).

MPF plays a role in XLX phosphorylation. As the substitution of all five serines to alanines completely abrogated the mobility shift of XLX, whereas MAPK inhibition only partially abrogated it, we hypothesized that the MPF/Cdc2 pathway also contributes to the phosphorylation of XLX. Cdc2/Cyclin B also phosphorylates serine residues followed by proline. We found that recombinant Cdc2/Cyclin B phosphorylated GST-XLXwt *in vitro*, whereas it did not phosphorylate GST-XLXS/A or GST-XLXS/D mutants (Figure 5b). In addition, T7-tagged XLX lacking the RING

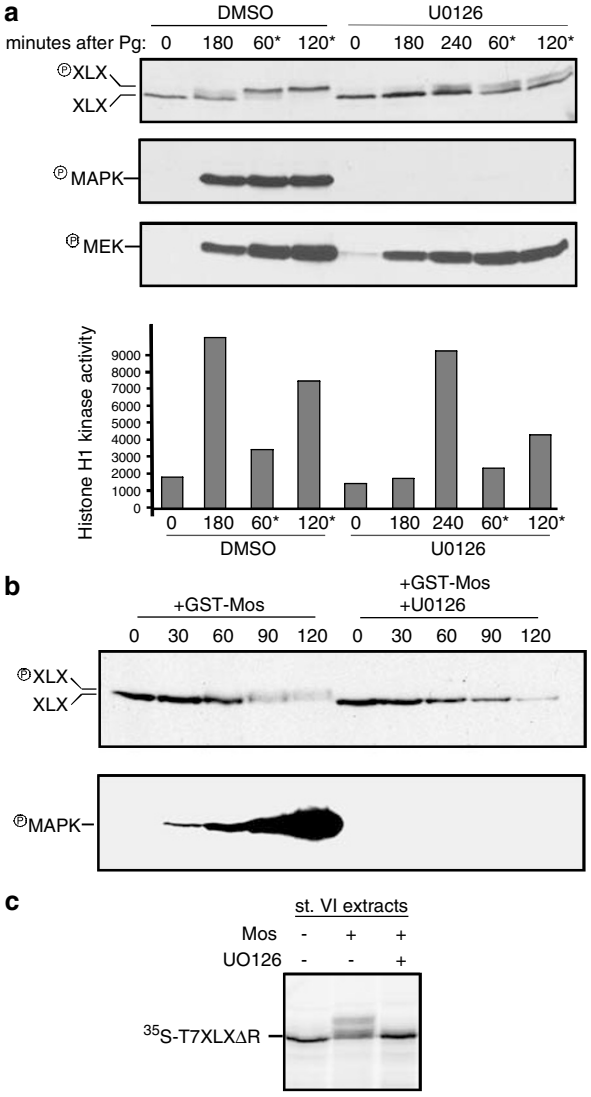

Figure 4 The MAPK pathway contributes to the phosphorylation of XLX during meiosis. (**a**) Oocytes were incubated with DMSO or U0126, a MEK inhibitor, before progesterone addition. GVBD, which was determined visually by the occurrence of a characteristic white spot, was delayed 60 min in the U0126-treated samples (for DMSO-treated oocytes, GVBD occurred at $t = 180$ min, whereas U0126-treated oocytes underwent GVBD at $t = 240$). Oocytes were collected at the indicated times following progesterone (Pg) addition, or after GVBD (*), and processed for SDS-PAGE and Western blot analysis. MAPK pathway activation was monitored by Western blot using antibodies specific for the phosphorylated form of MAPK (middle panel) or MEK (bottom panel). Cdc2/Cyclin B activity was monitored by histone H1 kinase activity (bar graph). (**b**) Extracts were generated from G2-arrested oocytes. Recombinant GST-Mos (50 μg/ml) was added to the extracts in the presence or absence of U0126. MAPK activation was monitored by Western blot using a phospho-specific MAPK antibody (bottom panel). XLX phosphorylation was monitored by Western blot analysis using purified XLX antibodies; the phosphorylated and unphosphorylated forms of XLX are indicated (top panel). (**c**) Exogenous XLX is phosphorylated in Mos-treated st. VI oocyte extracts. ^{35}S-XLXΔR was added to st. VI extracts from (**b**), and subjected to SDS-PAGE

domain, ^{35}S-T7ΔR-XLX, is phosphorylated in CSF extracts, and undergoes a mobility shift on SDS-PAGE (Figure 5c). However, when the extracts were treated with p21^{cip}, a specific inhibitor of cyclin-dependent kinases, phosphorylation of the exogenous XLX substrate was partially inhibited (Figure 5c). Taken together, these findings strongly suggest that in addition to the MAPK pathway, the MPF pathway contributes to full phosphorylation of XLX during meiosis.

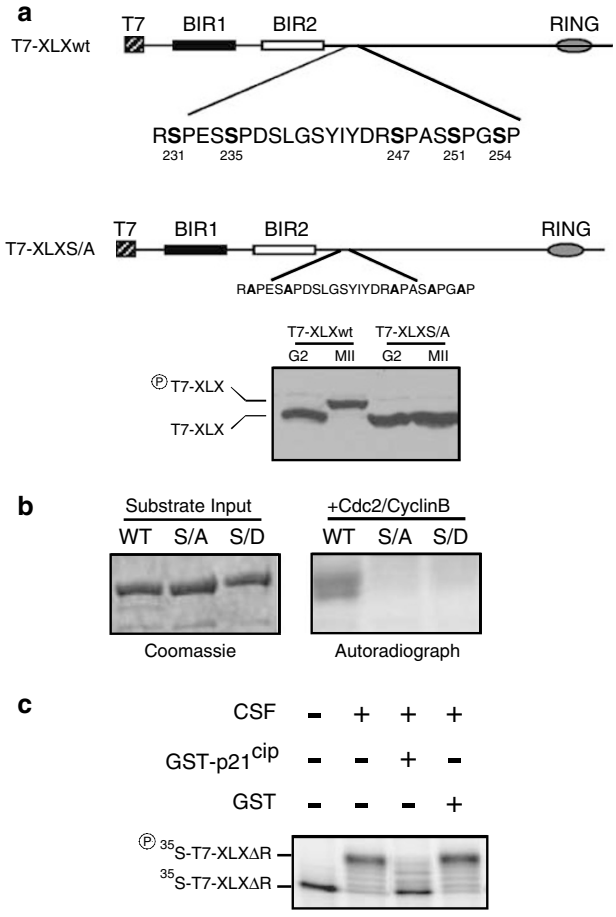

Figure 5 Identification of phosphorylated serines; Cdk activity contributes to XLX phosphorylation. (**a**) Schematic drawings of T7-tagged wild-type XLX (T7-XLXwt) or the serine-to-alanine mutant (T7-XLXS/A) are shown. Five serine-proline repeats were observed in the XLX protein sequence just C-terminal to the second BIR domain spanning amino acids 231–255. *In vitro* transcribed mRNA was generated from T7-XLXwt or T7-XLXS/A in which all five serines have been mutated to alanines. mRNAs were injected into st. VI oocytes, progesterone was added to induce maturation (MII) or not (G2), and oocytes were collected, and processed for Western blot analysis using an antibody against the T7 tag, to detect only exogenous XLX. (**b**) Recombinant Cdc2/Cyclin B was incubated with GST-XLXwt (WT) or phosphomutants GST-XLXS/A (S/A) and GST-XLXS/D (S/D) in the presence of [γ-^{32}P]ATP; products were analyzed by SDS-PAGE, Coomassie stained (left panel) followed by autoradiography (right panel). (**c**) ^{35}S-T7-XLXΔR was generated in reticulocyte lysate, bound to T7-antibody agarose beads, washed, incubated in CSF extract, and processed for SDS-PAGE and autoradiography. The Cdk inhibitor GST-p21^{cip} or GST as a control were added as indicated

To determine if phosphorylation of XLX affected its ability to inhibit caspase activity, we monitored ^{35}S-tPARP cleavage in caspase-active extracts supplemented with recombinant phosphomutants of XLX. We did not find any significant difference in the ability of non-phosphorylatable (GST-XLXS/A) or putative phosphomimic (GST-XLXS/D) mutants of XLX to inhibit caspase activity using this assay (Supplementary Figure 3a). In addition, we tested the GST-XLXS/D mutant as

both an E3 and as a substrate in *in vitro* ubiquitylation reactions (Supplementary Figure 3b). We did not detect a difference between the wild-type and the S/D mutant in these assays.

XLX cleavage is caspase-dependent; phosphorylation of XLX alters the cleavage product profile. Given the potential role of autoubiquitylation in regulating the level of IAP proteins, we wished to investigate the stability of the XLX protein in extracts. We found that XLX became highly unstable at the onset of spontaneous caspase activation in egg extracts following prolonged incubation at room temperature (Figure 6a). The appearance of faster migrating forms of XLX suggested that the protein may be cleaved in caspase-active extracts. To determine whether XLX is cleaved by caspases, ^{35}S-XLX was incubated in

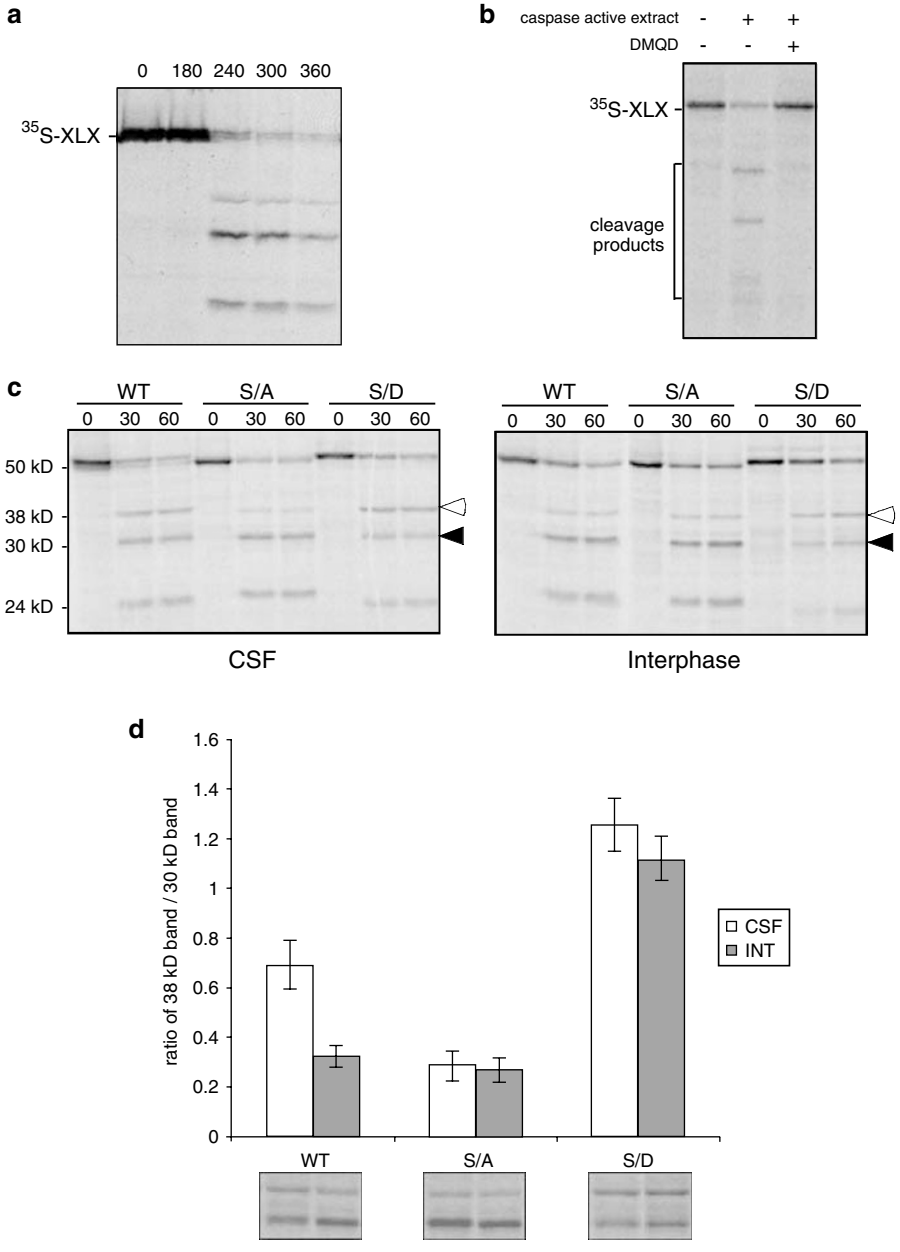

Figure 6 XLX is cleaved by caspases; cleavage products are altered by phosphorylation. (**a**) ^{35}S-XLX was added to interphase extracts at $t=0$, aliquots were taken at the indicated time points and analyzed by SDS-PAGE followed by autoradiography. Caspase activity was detected by tPARP cleavage at $t=240$ min (not shown). (**b**) ^{35}S-XLX was incubated in caspase-active extracts or in extracts in which caspase activity has been inhibited by the addition of a peptide caspase inhibitor, DMQD. Cleavage products were detected by SDS-PAGE followed by autoradiography. (**c**) ^{35}S-XLX (WT), ^{35}S-XLXS/A (S/A) or ^{35}S-XLXS/D (S/D) were pre-incubated in CSF extracts (left panel) or interphase extracts (right panel). Cytochrome *c* was then added and samples were collected at the indicated times and subjected to SDS-PAGE and autoradiography. (**d**) Bands from gels described in (**c**) were quantitated using the phosphorimager and ImageQuant software. Cleavage products were normalized against the total signal/lane. The mean ratio of the 38 kDa band (open arrowheads in (**c**)) over the 30 kDa band (closed arrowheads in (**c**)) is depicted in the bar graph using the $t=30$ min time point in either CSF-arrested extracts (CSF) or interphase extracts (INT). Error bars represent S.E.M. ($n=4$)

caspase-active extracts treated with or without peptide caspase inhibitor, DMQD. Inhibiting caspase activity was sufficient to block cleavage of XLX, suggesting that XLX is a substrate of a caspase, or that it is cleaved by a caspase-dependent protease (Figure 6b).

We considered the possibility that protease cleavage was sensitive to the phosphorylation state of XLX. To test this, ^{35}S-XLXwt, S/A, and S/D were incubated in CSF or interphase high-speed supernatant (HSS) extracts, and cytochrome *c* was added to induce caspase activation. Although all substrates tested were cleaved, a significant difference in the ratio of cleavage products was detected (Figure 6c,d). Full-length XLX migrates at 50 kDa. Each substrate yielded three detectable cleavage products, which migrate at approximately 38, 30, and 24 kDa on SDS-PAGE. We consistently observed an enrichment of the 38 kDa band when the substrate was either phosphorylated in CSF HSS extracts (wild-type XLX), or harbored phosphomimicking mutations (S/D) (Figure 6c). Wild-type XLX in interphase extracts and the non-phosphorylatable mutant (S/A) in both CSF and interphase extracts displayed a reduced proportion of the 38 kDa product (Figure 6c). To analyze the observed effect in a more quantitative manner, we performed phosphoimager quantitation of the bands, and graphed the ratio of the 38 kDa band to the 30 kDa band (Figure 6d). This analysis demonstrated that when XLX is not phosphorylated, either with S/A mutations or when wild type is incubated in interphase extracts, the 30 kDa band is favored over the 38 kDa band. Conversely, S/D mutations lead to a higher ratio of the 38 kDa band over the 30 kDa band. As we would expect, wild-type XLX phosphorylated in CSF extracts yields an intermediate ratio of 38/30 kDa product, presumably because the full-length substrate is not completely phosphorylated.

Discussion

XLX: An IAP family member. We found that in addition to exhibiting a maternal expression pattern, the IAP family member, XLX, is phosphorylated during oocyte maturation. To begin to understand the potential role of XLX in the regulation of either the M-phase-specific caspase resistance or the embryonic apoptotic delay, we first demonstrated that, like other IAPs, XLX exhibits caspase inhibition activity in an *in vitro* assay. We found that BIR2 of XLX was sufficient to inhibit caspase activity, and that a fragment of XLX lacking BIR domains was unable to inhibit caspase activity. We found that the anti-caspase activity of XLX was weak compared to human XIAP. This is consistent with a previous study in which the ability of XLX to inhibit spontaneous caspase activation in egg extracts was investigated and found to be less effective than *Xenopus* XIAP.[24] We did not see significant differences in the ability of RING-deleted XLX or XLX harboring mutations of its phosphorylation sites to inhibit caspase activity in this assay. However, we cannot rule out a role for either phosphorylation or the RING domain in the regulation of apoptosis inhibition in the embryo or oocyte *in vivo*. Although the caspase-active extracts generated from camptothecin-treated embryos provide a useful system in which to study the activity of some apoptotic components, this is a highly apoptotic environment that may not allow the detection of subtle differences in XLX activity. We therefore turned to *in vitro* approaches to dissect the activities of XLX.

We found that XLX exhibits autoubiquitylation activity *in vitro*. This is an activity XLX shares with other IAPs and highlights the potential importance of the RING domain in regulating the levels of apoptotic factors. We have found that XLX autoubiquitylation can occur intermolecularly. We have not tested the ability of XLX to ubiquitylate non-self substrates, but we hypothesize that such substrates exist, and if XLX behaves like others in the IAP family, we predict that XLX ubiquitylates other IAPs, caspases, IAP antagonists, or other cellular proteins.

MAPK- and MPF-dependent phosphorylation of XLX during oocyte maturation. We have shown that like interphase egg extracts, immature G2-arrested oocytes are more susceptible to cytochrome *c*-induced apoptosis than CSF-arrested oocytes. MAPK activity is also absent in G2-arrested oocytes, further supporting the role of this pathway in the meiotic inhibition of apoptosis. However, the targets of the MAPK pathway that provide the antiapoptotic activity have remained elusive. We have identified a target of the MAPK pathway, XLX. Full phosphorylation of XLX also requires Cdk activity. We have identified the residues that become phosphorylated; the serines are clustered together between BIR2 and the RING domain and overlap with a putative PEST sequence.[24] The studies described here demonstrate for the first time that an IAP can be a substrate for a kinase in the MAPK pathway. This novel mode of regulation of an IAP family member opens a new window into the study of apoptotic regulation within a developmental and cell cycle-dependent context.

Possible role of XLX phosphorylation. The role of phosphorylation in the function of XLX is not yet clear. It is possible that phosphorylation could induce a change in XLX structure, stability, localization, or binding partner specificity. We did not detect a difference in the ability of XLX phosphomutants to inhibit caspase activity. In addition, we have investigated the role of XLX in meiotic maturation and have found no detectable changes in the timing or occurrence of GVBD when XLX is overexpressed, depeleted, or when phosphomutants are expressed (data not shown). We also tested the ability of XLX to autoubiquitylate when the targeted serines are mutated to aspartic acids and found no change *in vitro*. As regulation of XLX stability *in vivo* may not depend on autoubiquitylation activity, we continued to test the stability of XLX protein under various conditions. We have shown that XLX is cleaved in a caspase-dependent manner in apoptotic extracts. Although the significance of the cleavage of XLX with respect to overall cell survival remains to be determined, we have observed a phosphorylation-specific difference in the profile of cleavage products of XLX. Specifically, when XLX is phosphorylated or when XLX phosphorylation sites are mutated to aspartic acids, the 38 kDa cleavage product is favored over the 30 kDa product. The significance of this difference requires further analysis; however, we

hypothesize that the cleavage product profile change could indicate a change in the structure or binding partner of XLX that alters the accessibility of the protease to the cleavage site(s). Alternatively, the cleavage products themselves could be uniquely regulated by phosphorylation. Further studies are needed to elucidate the significance of caspase-dependent XLX cleavage and phosphorylation.

Materials and Methods

Generation of XLX mutants. BIR-encoding cDNA fragments were cloned from unfertilized eggs using degenerate oligonucleotides designed based on the conserved sequence of the BIR. The fragment was used as a hybridization probe to screen a *Xenopus laevis* oocyte λ-ZAP cDNA library. The isolated clone contains a 1591 bp cDNA, with an open reading frame of 1200 bp. The sequence is identical to the published sequence of XLX.[23] Full-length XLX was subcloned into both pGEX-2T and pET21 vectors, generating N-terminal GST and T7 fusions, respectively. Deletion mutants were generated by PCR as follows: GST-XLXΔR and T7-XLXΔR contain the wild-type sequence with a stop codon at Gln345. GST-XLX 133-307 encodes GST fused to XLX Asp133 through Ala352 followed by a stop codon. GST-XLXBIR2 contains Asp133 through Ile222 followed by a stop codon. GST-XLX214-400 contains the C-terminal fragment of XLX starting at Leu214 fused to GST at the N-terminus. Phosphomutants were generated by PCR using primers in various combinations (see Supplementary Materials and Methods) between the *Stu*I site at bp 652 and *Pst*I at bp 807. GST-XLXS/A, T7-XLXS/A, GST-XLXS/D, and T7-XLXS/D contain the full-length XLX sequence with the following serines mutated to alanines or aspartic acids respectively: Ser231, Ser235, Ser247, Ser251, Ser254. All substitutions were confirmed by sequence analysis. The *Stu*I/*Pst*I fragment was then subcloned into T7-XLXΔR to generate phosphomutants lacking the RING domain. Individual Ser/Ala mutations were also generated. ^{35}S-labeled tPARP and T7-fused XLX clones were generated using the Promega coupled transcription–translation reticulocyte lysate system according to the protocol supplied.

Protein purification. GST-XLXwt and all GST-XLX mutant proteins were expressed in BL21 bacteria during a 12 h induction with 0.05 mM IPTG at 28°C. The bacteria were lysed in STE buffer (10 mM Tris-HCl (pH 8.0), 150 mM NaCl, 1 mM EDTA, and 5 mM DTT). 0.75% *N*-lauryl sarcosine and 3% Triton X-100 were added and lysates were sonicated; the insoluble fraction was removed by centrifugation at 10 000 $\times$ *g*. Following incubation of lysates with glutathione-agarose for 4 h at 4°C, beads were washed with 20 mM Tris-HCl (pH 8.0), 500 mM NaCl, 1 mM EDTA, and 5 mM DTT. The protein was eluted in 20 mM Tris (pH 8.8), 150 mM NaCl, 0.1 mM EDTA, 10 mM DTT, 0.1% Triton, and 50 mM glutathione. The eluted protein was then dialyzed in 20 mM Tris (pH 8.0), 150 mM NaCl, 0.1 mM EDTA, and 1 mM DTT. GST-Mos, a gift from Jim Maller, was produced in Sf9 baculovirus cells, and purified as described previously.[31] GST-p21^{Cip} and Cdc2/Cyclin B were generated and purified as described previously.[32]

Antibodies. Polyclonal antibodies were generated in rabbit against full-length GST-XLXwt and subsequently affinity purified as follows. GST or GST-XLXBIR2 was crosslinked to glutathione sepharose beads as described previously.[33] Crude rabbit serum was then incubated with the GST-fused beads for 2–3 h at 4°C, the flow-through was collected, and incubated with beads fused to GST-XLXBIR2. XLX-specific antibodies were then eluted with 100 mM glycine-HCl (pH 2.5), and neutralized with 1 M Tris base. Antibodies against phosphorylated MAPK, MAPK, and phosphorylated MEK were purchased from Cell Signaling Technology. T7 antibody was purchased from Novagen. Polyclonal MCM2 antibody was generated in rabbit.[34]

Oocytes, embryos, and egg extracts. Stage VI oocytes and metaphase II oocytes were obtained as in Jessus *et al.*[35] Oocytes were homogenized in EB (80 mM β-glycerophosphate (pH 7.3), 15 mM $MgCl_2$, 20 mM EGTA, 10 mM DTT, 10 μg/ml each of pepstatin, chymostatin, and leupeptin). For MEK inhibition, oocytes were incubated in 50 μM U0126 for 30 min before and for the duration of progesterone incubation. *In vitro* transcribed mRNA was prepared using the mMessage mMachine kit from Ambion and 10 nl of 100 pg/nl were microinjected into st. VI oocytes. Either 10 or 25 ng (total) of sense (A + B) and antisense (A + B) oligonucleotides were injected into st. VI oocytes. The sequences of the oligonucleotides are as follows: sense A: CAGTATGAGGAGCGAGGC; sense B: GAGAATGAGTCGCTGGTC; antisense A: GCCTCGCTCCTCATACTG; antisense B: GACCAGCGACTCATTCTC. St. VI oocyte extracts: crude extracts from st. VI oocytes were generated according to Karaiskou *et al.*[36] GST-Mos was added at a final concentration of 50 μg/ml. *Xenopus laevis* embryos were obtained by *in vitro* fertilization and cultured using standard methods. Embryos were staged according to Nieuwkoop PDaJF.[37] Low-speed supernatant (LSS) CSF-arrested and interphase extracts were freshly prepared as in Murray.[38] HSS extracts were generated by further centrifugation of CSF-LSS or interphase-LSS at 250 000 $\times$ *g*; the cytosolic fraction was collected. Recombinant λ-phosphatase was purchased from New England Biolabs.

Kinase assays. Histone H1 kinase activity in oocytes and extracts were performed as described previously.[39] *In vitro* phosphorylation of XLX by Cdc2/Cyclin B was carried out as above using 1 μg of the substrate, recombinant GST-XLXwt, or phosphomutants. Products were analyzed by SDS-PAGE and autoradiography.

Caspase activity assay. Fertilized embryos were treated with 30 μM camptothecin before st. 3 for 1 h at room temperature, and subsequently rinsed with 1 $\times$ MMR; apoptotic embryos were collected at st. 10.5. Embryos were rinsed in EB, crushed by centrifugation at 10 000 r.p.m. for 10 min, and the cytoplasmic layer was collected and snap-frozen on liquid nitrogen. Extracts were then thawed and diluted 1 : 1 in EB. Recombinant protein was added to a final concentration of (1–3 μM) or DMQD was added at a final concentration of 25 μM, 1/8 volume ^{35}S-tPARP transcription/translation reaction was added, samples were removed at the time points indicated and subjected to SDS-PAGE followed by autoradiography and quantification with ImageQuant software.

Ubiquitylation assays. ^{35}S-labeled T7-fused XLXΔR generated in reticulocyte lysate was bound to T7-antibody agarose beads (Novagen). The beads were then equilibrated with ubiquitylation buffer (50 mM Tris (pH 7.5), 2 mM ATP, 5 mM $MgCl_2$, and 2 mM DTT) and the following components were added: ubiquitin-activating enzyme E1, 200 ng, UbcH5b, 150 ng, His-6-ubiquitin 10 μg (all from Boston Biochem), and 250 ng GST-XLX as the E3. Ubiquitylation of the substrate was analyzed by SDS-PAGE followed by autoradiography.

Acknowledgements. We are grateful to members of the Gautier laboratory, especially M. Di Virgilio, Dr. C. Ying, R. Sattler, and Dr. A. Dupre for helpful discussions and critical reading of the paper.

1. Vaux DL, Silke J. IAPs, RINGs ubiquitylation. *Nat Rev Mol Cell Biol* 2005; **6**: 287–297.
2. Harlin H, Reffey SB, Duckett CS, Lindsten T, Thompson CB. Characterization of XIAP-deficient mice. *Mol Cell Biol* 2001; **21**: 3604–3608.
3. Wang SL, Hawkins CJ, Yoo SJ, Muller HA, Hay BA. The *Drosophila* caspase inhibitor DIAP1 is essential for cell survival and is negatively regulated by HID. *Cell* 1999; **98**: 453–463.
4. Eckelman BP, Salvesen GS. The human anti-apoptotic proteins cIAP1 and cIAP2 bind but do not inhibit caspases. *J Biol Chem* 2006; **281**: 3254–3260.
5. Scott FL, Denault JB, Riedl SJ, Shin H, Renatus M, Salvesen GS. XIAP inhibits caspase-3 and -7 using two binding sites: evolutionarily conserved mechanism of IAPs. *EMBO J* 2005; **24**: 645–655.
6. Shiozaki EN, Chai J, Rigotti DJ, Riedl SJ, Li P, Srinivasula SM *et al.* Mechanism of XIAP-mediated inhibition of caspase-9. *Mol Cell* 2003; **11**: 519–527.
7. Shin H, Renatus M, Eckelman BP, Nunes VA, Sampaio CA, Salvesen GS. The BIR domain of IAP-like protein 2 is conformationally unstable: implications for caspase inhibition. *Biochem J* 2005; **385** (Part 1): 1–10.
8. Vucic D, Franklin MC, Wallweber HJ, Das K, Eckelman BP, Shin H *et al.* Engineering ML-IAP to produce an extraordinarily potent caspase 9 inhibitor: implications for Smac-dependent anti-apoptotic activity of ML-IAP. *Biochem J* 2005; **385** (Part 1): 11–20.
9. Duckett CS. IAP proteins: sticking it to Smac. *Biochem J* 2005; **385** (Part 1): e1–e2.
10. Silke J, Hawkins CJ, Ekert PG, Chew J, Day CL, Pakusch M *et al.* The anti-apoptotic activity of XIAP is retained upon mutation of both the caspase 3- and caspase 9-interacting sites. *J Cell Biol* 2002; **157**: 115–124.
11. Wilkinson JC, Wilkinson AS, Scott FL, Csomos RA, Salvesen GS, Duckett CS. Neutralization of Smac/Diablo by inhibitors of apoptosis (IAPs). A caspase-independent mechanism for apoptotic inhibition. *J Biol Chem* 2004; **279**: 51082–51090.
12. Dan HC, Sun M, Kaneko S, Feldman RI, Nicosia SV, Wang HG *et al.* Akt phosphorylation and stabilization of X-linked inhibitor of apoptosis protein (XIAP). *J Biol Chem* 2004; **279**: 5405–5412.
13. Harvey KF, Pfleger CM, Hariharan IK. The *Drosophila* Mst ortholog, hippo, restricts growth and cell proliferation and promotes apoptosis. *Cell* 2003; **114**: 457–467.

14. Pantalacci S, Tapon N, Leopold P. The Salvador partner Hippo promotes apoptosis and cell-cycle exit in *Drosophila*. *Nat Cell Biol* 2003; **5**: 921–927.
15. Ditzel M, Wilson R, Tenev T, Zachariou A, Paul A, Deas E *et al*. Degradation of DIAP1 by the N-end rule pathway is essential for regulating apoptosis. *Nat Cell Biol* 2003; **5**: 467–473.
16. Clem RJ, Sheu TT, Richter BW, He WW, Thornberry NA, Duckett CS *et al*. c-IAP1 is cleaved by caspases to produce a proapoptotic C-terminal fragment. *J Biol Chem* 2001; **276**: 7602–7608.
17. Deveraux QL, Leo E, Stennicke HR, Welsh K, Salvesen GS, Reed JC. Cleavage of human inhibitor of apoptosis protein XIAP results in fragments with distinct specificities for caspases. *EMBO J* 1999; **18**: 5242–5251.
18. Nachmias B, Ashhab Y, Bucholtz V, Drize O, Kadouri L, Lotem M *et al*. Caspase-mediated cleavage converts Livin from an antiapoptotic to a proapoptotic factor: implications for drug-resistant melanoma. *Cancer Res* 2003; **63**: 6340–6349.
19. Newmeyer DD, Farschon DM, Reed JC. Cell-free apoptosis in *Xenopus* egg extracts: inhibition by Bcl-2 and requirement for an organelle fraction enriched in mitochondria. *Cell* 1994; **79**: 353–364.
20. Tashker JS, Olson M, Kornbluth S. Post-cytochrome C protection from apoptosis conferred by a MAPK pathway in *Xenopus* egg extracts. *Mol Biol Cell* 2002; **13**: 393–401.
21. Faure S, Vigneron S, Doree M, Morin N. A member of the Ste20/PAK family of protein kinases is involved in both arrest of *Xenopus* oocytes at G2/prophase of the first meiotic cell cycle and in prevention of apoptosis. *EMBO J* 1997; **16**: 5550–5561.
22. Stefanis L, Park DS, Yan CY, Farinelli SE, Troy CM, Shelanski ML *et al*. Induction of CPP32-like activity in PC12 cells by withdrawal of trophic support. Dissociation from apoptosis. *J Biol Chem* 1996; **271**: 30663–30671.
23. Holley CL, Olson MR, Colon-Ramos DA, Kornbluth S. Reaper eliminates IAP proteins through stimulated IAP degradation and generalized translational inhibition. *Nat Cell Biol* 2002; **4**: 439–444.
24. Tsuchiya Y, Murai S, Yamashita S. Apoptosis-inhibiting activities of BIR family proteins in *Xenopus* egg extracts. *FEBS J* 2005; **272**: 2237–2250.
25. Greenwood J, Gautier J. From oogenesis through gastrulation: developmental regulation of apoptosis. *Semin Cell Dev Biol* 2005; **16**: 215–224.
26. Anderson JA, Lewellyn AL, Maller JL. Ionizing radiation induces apoptosis and elevates cyclin A1-Cdk2 activity before but not after the midblastula transition in *Xenopus*. *Mol Biol Cell* 1997; **8**: 1195–1206.
27. Finkielstein CV, Lewellyn AL, Maller JL. The midblastula transition in *Xenopus* embryos activates multiple pathways to prevent apoptosis in response to DNA damage. *Proc Natl Acad Sci USA* 2001; **98**: 1006–1011.
28. Hensey C, Gautier J. A developmental timer that regulates apoptosis at the onset of gastrulation. *Mech Dev* 1997; **69**: 183–195.
29. Sible JC, Anderson JA, Lewellyn AL, Maller JL. Zygotic transcription is required to block a maternal program of apoptosis in *Xenopus* embryos. *Dev Biol* 1997; **189**: 335–346.
30. Gross SD, Schwab MS, Taieb FE, Lewellyn AL, Qian YW, Maller JL. The critical role of the MAP kinase pathway in meiosis II in *Xenopus* oocytes is mediated by p90(Rsk). *Curr Biol* 2000; **10**: 430–438.
31. Roy LM, Haccard O, Izumi T, Lattes BG, Lewellyn AL, Maller JL. Mos proto-oncogene function during oocyte maturation in *Xenopus*. *Oncogene* 1996; **12**: 2203–2211.
32. Harper JW, Elledge SJ, Keyomarsi K, Dynlacht B, Tsai LH, Zhang P *et al*. Inhibition of cyclin-dependent kinases by p21. *Mol Biol Cell* 1995; **6**: 387–400.
33. Bar-Peled M, Raikhel NV. A method for isolation and purification of specific antibodies to a protein fused to the GST. *Anal Biochem* 1996; **241**: 140–142.
34. Ying CY, Gautier J. The ATPase activity of MCM2-7 is dispensable for pre-RC assembly but is required for DNA unwinding. *EMBO J* 2005; **24**: 4334–4344.
35. Jessus C, Thibier C, Ozon R. Levels of microtubules during the meiotic maturation of the *Xenopus* oocyte. *J Cell Sci* 1987; **87** (Part 5): 705–712.
36. Karaiskou A, Cayla X, Haccard O, Jessus C, Ozon R. MPF amplification in *Xenopus* oocyte extracts depends on a two-step activation of cdc25 phosphatase. *Exp Cell Res* 1998; **244**: 491–500.
37. Nieuwkoop PDaJF *Normal table of Xenopus laevis* 1967.
38. Murray AW. Cell cycle extracts. *Methods Cell Biol* 1991; **36**: 581–605.
39. Furuno N, Nishizawa M, Okazaki K, Tanaka H, Iwashita J, Nakajo N *et al*. Suppression of DNA replication via Mos function during meiotic divisions in *Xenopus* oocytes. *EMBO J* 1994; **13**: 2399–2410.

Supplementary Information accompanies the paper on Cell Death and Differentiation website (http://www.nature.com/cdd)